

# Catalytic Solid-Phase Seeding of Silicon Nanowires by Nickel Nanocrystals in Organic Solvents

Hsing-Yu Tuan, Doh C. Lee, Tobias Hanrath, and Brian A. Korgel\*

Department of Chemical Engineering, Texas Materials Institute, Center for Nano- and Molecular Science and Technology, The University of Texas at Austin, Austin, Texas 78712-1062

Received January 17, 2005

## ABSTRACT

Colloidal nickel (Ni) nanocrystals were used to direct the synthesis of crystalline silicon (Si) nanowires in an organic solvent. The reaction temperatures ranged from 400 °C to 520 °C with pressures from 14.3 to 23.4 MPa, conditions that are well above the critical point of the solvent. The Ni nanocrystals play two roles in the synthesis: (1) Ni catalyzes the decomposition of the silicon precursors, i.e., arylsilanes, alkylsilanes, and trisilane, to silicon; (2) Ni nanocrystals induce silicon crystallization through the *solid-phase* alloying of Si in the Ni seeds. We call this nanowire growth mechanism supercritical fluid–solid–solid (SFSS) synthesis.

**Introduction.** Silicon's significant crystallization energy barrier and prevalence to form stable organosilanes make “conventional” colloidal solution-phase syntheses in high boiling point coordinating solvents ineffective for Si nanomaterials. To overcome these fundamental limitations, we have employed pressurized solvents and a “VLS” approach to synthesize crystalline Si nanowires by decomposing diphenylsilane in hexane at ~450 °C and ~250 bar in the presence of dodecanethiol-coated gold nanocrystals.<sup>1–3</sup> Solution-phase approaches to VLS nanowire growth<sup>1,4–7</sup> have the potential for much higher production rates than gas-phase chemical vapor deposition (CVD)<sup>8–10</sup> since the synthesis can be carried out homogeneously in a continuous flow-through reactor as opposed to on a substrate in a batch process.<sup>4,11</sup> Reaction temperatures can be reached in pressurized solvents between 350 °C and 650 °C, which, although extending the accessible temperature range for solution-phase chemistry, are still relatively cold with respect to accessible gas-phase temperatures. The Au/Si eutectic temperature (363 °C) is easily reachable, but Au forms deep carrier traps in Si and must be avoided for electronic applications. Metals compatible with Si electronics, such as Ti, Co, Fe, and Ni exhibit eutectic temperatures that greatly exceed the decomposition temperatures of organic solvents (~650 °C).<sup>12</sup> However, many of these metals, including Ti, Co, and Ni, form silicides with the potential for *solid-phase* seeding of nanowires. In the gas phase, Kamins and co-workers demonstrated solid-phase seeding of Si nanowires by Ti particles at 640 °C.<sup>10</sup>

Again, synthetic temperatures in this range are not accessible in organic solvents. However, it is well-known in the microelectronics industry that annealing a Si wafer with a layer of Ni at 400 °C promotes the solid-phase alloying and formation of nickel silicide, a process used by Intel to achieve good local source-drain contacts in transistors.<sup>13,14</sup> Here we demonstrate the first example of solid-phase metal particle-seeding of semiconductor nanowires in solution, using nickel (Ni) nanocrystals to promote Si nanowires from silane precursors in organic solvents at ~460 °C and ~20 MPa. The Ni nanocrystals induce crystallization and *additionally* catalyze precursor (i.e., arylsilanes, alkylsilanes, trisilane) decomposition.

Figure 1 shows SEM and TEM images of Si nanowires synthesized using monophenylsilane (MPS) as a precursor in toluene at 23.4 MPa in the presence of Ni nanocrystals (see Supporting Information for experimental details). The reaction temperature has a significant influence on the quality of the nanowires. The best growth temperature at this pressure is 460 °C, producing straight crystalline nanowires longer than 10 μm with Si diamond cubic crystal structure and few dislocation defects (Figure 1c). The nanowires exhibit predominantly the ⟨110⟩ growth direction (Figures 1g, 1h, 1i). Although TEM images of the nanowire surface show a significant amount of roughness, the diameter fluctuates by only ~1 nm along the entire length of the nanowire with negligible sidewall growth.

The inset in Figure 1c shows an example of a Ni seed particle at the tip of a nanowire. Ni nanocrystals with 5~6 nm diameter produced nanowires with slightly larger diam-

\* Corresponding author: Phone: (512) 471-5633; FAX: (512) 471-7060; email: korgel@mail.che.utexas.edu.

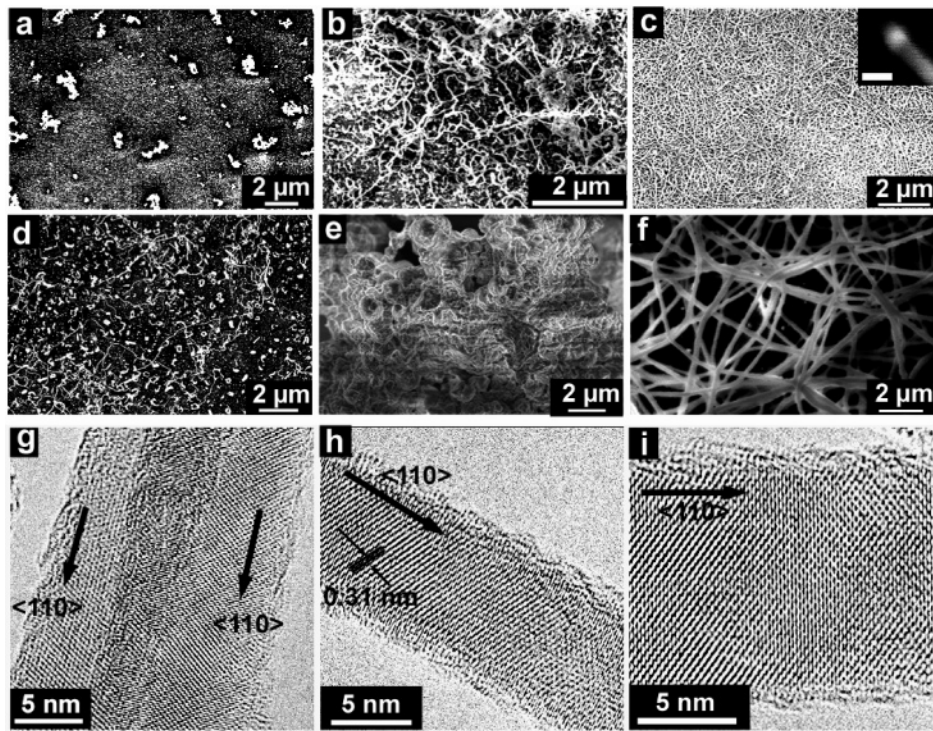


**Figure 1.** HRSEM images of Si nanowires synthesized from MPS in toluene at 23.4 MPa (10 min, 27.4 mM MPS,  $[Si]/[Ni] = 100$ ) at (a) 340 °C, (b) 400 °C, (c) 460 °C, (d) 520 °C, (e) 580 °C, and (f) 460 °C. EDS of the product shows an abundance of Si. Inset in (c) shows a Ni particle at the Si nanowire tip [scale bar is 25 nm]. HRTEM images (g, h, i) of Si nanowires seeded by Ni nanocrystals in toluene at 460 °C, 23.4 MPa (10 min, 27.4 mM MPS,  $[Si]/[Ni] = 100$ ). The nanowires exhibit the  $\langle 110 \rangle$  growth direction.

eter, between 7 and 25 nm. The Ni nanocrystals promote Si nanowire growth by a solid-phase seeding mechanism that we call supercritical fluid–solid–solid (SFSS) growth. There is a high solid Si solubility in Ni at 460 °C,<sup>13</sup> and the small diameter of the seed particles enables rapid solubilization within the entire nanocrystal core to promote Si crystallization. Below  $\sim 400$  °C, nanowires do not form (Figure 1a), and between 400–450 °C (Figure 1b) the synthesis yields curly Si nanowires riddled with defects. These temperatures are most likely too low for rapid Si saturation of the Ni seed particles needed for nanowire growth.<sup>2</sup> However, reaction temperatures exceeding 500 °C led to low yields of nanowires with poor crystallinity and a large amount of particulate byproduct. At 520 °C (Figure 1d), only very few poor quality nanowires are produced. At 580 °C (Figure 1e) and above, nanowires do not form. At the higher reaction temperatures, homogeneous Si particulate formation competes with heterogeneous nanowire growth, as has been observed in the SFLS process as well.<sup>2</sup>

We have also found that in addition to promoting Si crystallization, the Ni nanocrystals catalyze the decomposition of silane precursors, such as alkylsilanes and trisilane, that do not yield crystalline nanowires in the Au nanocrystal-seeded SFLS process due to their poor reactivity. Figures 2 and 3 show Si nanowires synthesized from octylsilane and trisilane using Ni nanocrystals. We have found it impossible to thermally decompose these precursors to *crystalline* Si in organic solvents, even in the presence of Au nanocrystals (see Figures 2a and 3a), due to the thermal stability of the Si–C and Si–Si bonds in alkylsilanes and trisilane. The

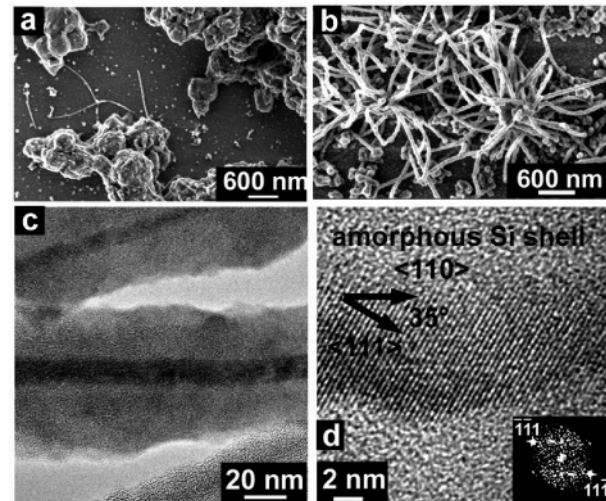


**Figure 2.** Si synthesized with octylsilane in toluene at 17.9 MPa and 460 °C: SEM images of product obtained using (a) Au and (b) Ni nanocrystals ( $[Si]/[Ni] = 100$ ) and (c,d) TEM images of the Si nanowires synthesized by Ni-seeded SFSS from octylsilane. In (c) and (d), note the characteristic amorphous shell that coats the crystalline core that results from sidewall deposition.

Si–C bond in octylsilane is very stable and does not undergo thermolysis at temperatures lower than  $\sim 500$  °C. Furthermore, the alkyl moiety in octylsilane is not kinetically labile like the phenyl group in arylsilanes and cannot disproportionate to yield silane. In trisilane, hydrogen atoms dissociate easily from the molecule but the Si–Si bonds do not cleave at temperatures accessible in organic solvents. Thermal decomposition of trisilane in toluene at 460 °C yields very

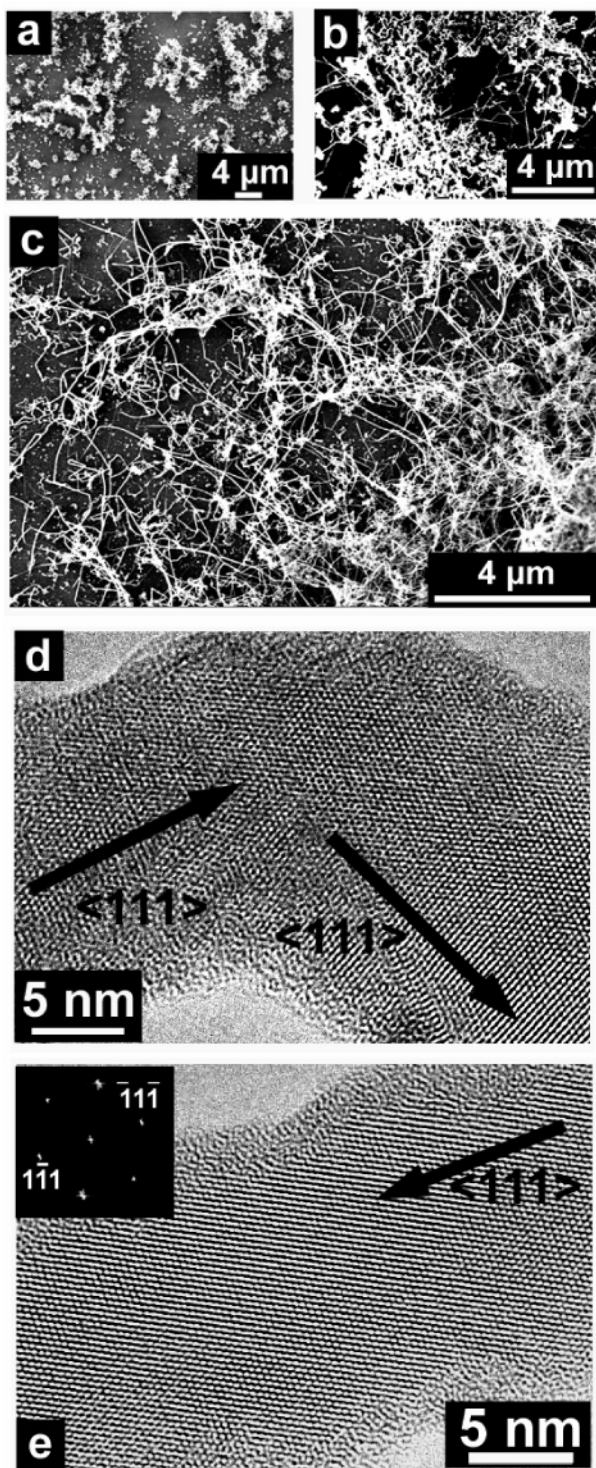


**Figure 3.** Si produced from trisilane in hexane at 14.3 MPa and 450 °C: SEM images of product obtained using (a) Au nanocrystals ( $[Si]/[Au] = 5$ ), (b) Ni nanocrystals ( $[Si]/[Ni] = 10$ ), and (c) Ni nanocrystals ( $[Si]/[Ni] = 5$ ). (d,e) TEM images of nanowires obtained from trisilane in the presence of Ni nanocrystals exhibiting crystalline cores. In contrast to nanowires grown from MPS and octylsilane, the nanowires shown here have grown in the  $\langle 111 \rangle$  direction.

reactive Si trimers that homogeneously nucleate into amorphous Si colloids<sup>15</sup> and do not produce nanowires by Au-seeded SFLS. Apparently, the Si–Si bonds must be “cracked” in order to form nanowires. Ni nanocrystals promote Si

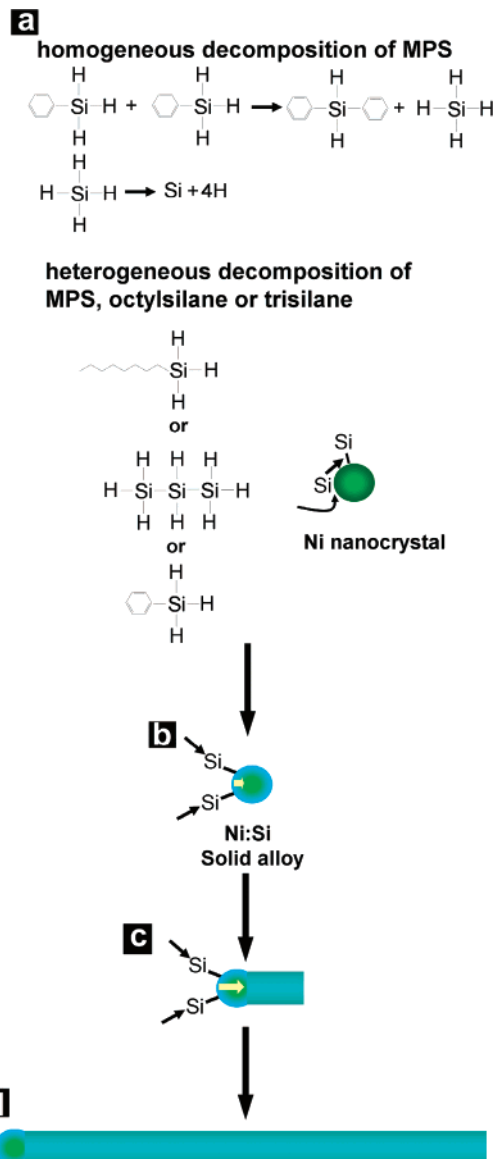


**Figure 4.** Si nanowire growth via SFSS. (a) Homogeneous MPS decomposition occurring by disproportionation versus heterogeneous MPS, octylsilane, and trisilane decomposition catalyzed by the Ni surface. (b) Si atoms diffuse into the Ni nanocrystal until reaching saturation. (c) Silicon nanowire nucleates and crystallizes from the Ni/Si alloy interface, growing to produce the high aspect ratio nanowire illustrated in (d).

nanowire growth with relatively high yield from both octylsilane and trisilane.

Although the Si nanowires formed using octylsilane and trisilane are crystalline and relatively long, the quality of the wires is still not as high as those obtained with MPS. In contrast to MPS, both octylsilane and trisilane gave significant amounts of amorphous sidewall deposition. The more significant sidewall deposition from trisilane is certainly expected, as it undergoes rapid dehydrogenation to a very reactive “bare” Si trimer that will “stick” to anything it sees in solution.<sup>15</sup> Sidewall growth could be eliminated to some extent by using higher  $[Ni]/[Si]$ , with the best Si nanowires obtained from trisilane by using nearly 2 orders of magnitude larger  $[Ni]/[Si]$  than in the case of MPS (5 vs 100). One drawback with using very high  $[Ni]/[Si]$  is that the Si supply

to the metal seeds can become starved, which leads to crystallographic defects.<sup>2</sup> Sidewall-deposited Si from octylsilane is amorphous, but in contrast to trisilane, most likely contains significant carbon contamination. Octylsilane dehydrogenation may happen quite rapidly at 460 °C, however, the Si–C bond is thermally very stable and at these temperatures in supercritical toluene, and octylsilane tends to dimerize and form thermally stable oligomers. For example, most of the particulates in Figure 2a are large precipitates of aggregated oligomers and amorphous mixtures of carbon and silicon. Therefore, to produce crystalline Si nanowires from octylsilane, the Ni nanocrystals must first catalyze its decomposition to make crystalline nanowires.

Figure 4 provides an overview of the Ni-seeded SFSS synthetic mechanism. Octylsilane and trisilane require heterogeneous catalytic decomposition on the Ni surface to form nanowires, whereas MPS can undergo homogeneous disproportionation to silane, which can then give rise to nanowire growth. Nanowires produced by SFLS and SFSS from MPS are of relatively high quality with little sidewall growth because of the low precursor reactivity, which results in Si formation isolated to the metal seed particle surface. This study highlights the importance of the precursor decomposition kinetics on the quality of nanowires grown by the VLS approach. The growth temperature must be high enough to sustain precursor decomposition and nanowire crystallization, but not so high that sidewall growth occurs to an appreciable extent. In CVD VLS, the precursor reactivity can be decreased and balanced by feeding in additives, such as H<sub>2</sub> in the case of Au-seeded Ge nanowire growth from GeH<sub>4</sub>.<sup>8</sup> In solution, additional species can be added to the reactor; however, much less is known about the decomposition kinetics of organosilanes (and organometallics in general) in high-pressure solvents, and finding the appropriate nanowire growth conditions is still a challenge. Nonetheless, we have demonstrated in this study that reaction conditions can be optimized to produce nanowires

in solution with equal or better quality than those synthesized by gas-phase methods, with the potential for scale-up and high throughput synthesis.

**Acknowledgment.** We thank the National Science Foundation, the Welch Foundation, and the Advanced Materials Research Center for financial support of this research. We also thank J. P. Zhou for assistance with the operation of HRTEM.

**Supporting Information Available:** Experimental details and additional characterization of Ni nanocrystals and Si nanowires. This material is available free of charge via the Internet at <http://pubs.acs.org>.

## References

- (1) Holmes, J. D.; Johnston, K. P.; Doty, R. C.; Korgel, B. A. *Science* **2000**, *287*, 1471–1473.
- (2) Lu, X.; Hanrath, T.; Johnston, K. P.; Korgel, B. A. *Nano Lett.* **2003**, *3*, 93–99.
- (3) Hanrath, T.; Korgel, B. A. *Adv. Mater.* **2003**, *15*, 437–440.
- (4) Lee, D. C.; Mikulec, F. V.; Korgel, B. A. *J. Am. Chem. Soc.* **2004**, *126*, 4951–4957.
- (5) Hanrath, T.; Korgel, B. A. *J. Am. Chem. Soc.* **2002**, *124*, 1424–1429.
- (6) Grebinski, J. W.; Hull, K. L.; Zhang, J.; Kosel, T. H.; Kuno, M. *Chem. Mater.* **2004**, *16*, 5260–5272.
- (7) Yu, H.; Buhr, W. E. *Adv. Mater.* **2003**, *15*, 416–419.
- (8) Wang, D.; Dai, H. *Angew. Chem., Int. Ed.* **2002**, *41*, 4783–4786.
- (9) Cui, Y.; Lauhon, L. J.; Gudiksen, M. S.; Wang, J.; Lieber, C. M. *App. Phys. Lett.* **2001**, *78*, 2214–2216.
- (10) Kamins, T. I.; Williams, S. R.; Basile, D. P.; Hesjedal, T.; Harris, J. S. *J. Appl. Phys.* **2001**, *89*, 1008–1016.
- (11) Shah, P. S.; Hanrath, T.; Johnston, K. P.; Korgel, B. A. *J. Phys. Chem. B* **2004**, *108*, 9574–9587.
- (12) *Binary Alloy Phase Diagram*, 2nd ed.; ASM International: Materials Park, OH, 1990; Vol. 1.
- (13) D'Heurle, F.; Petersson, C. S.; Baglin, J. E. E.; La Placa, S. J.; Wong, C. Y. *J. Appl. Phys.* **1984**, *55*, 4208–18.
- (14) Chi, D. Z.; Mangelinck, D.; Zuruzi, A. S.; Wong, A. S. W.; Lahiri, S. K. *J. Electron. Mater.* **2001**, *30*, 1483–1488.
- (15) Pell, L. E.; Schriener, A. D.; Mikulec, F. V.; Korgel, B. A. *Langmuir* **2004**, *20*, 6546–6548.

NL050099D